III. RESULTS

3.1 Multiple mechanisms mediate glia-induced synaptogenesis in RGCs

Starting from the publication of Nägler et al. (2001), which showed that soluble glial-derived factors enhance the formation and efficacy of synapses in cultured RGCs, and of Mauch et al. (2001), which identified cholesterol as one of this glia derived factors, I studied how cholesterol and other secreted factors from glial cells influence synapse development in microcultures of highly purified rat RGCs. To separate effects mediated by GCM and by cholesterol, which is contained in GCM in form of lipoproteins (LaDu et al., 1998; DeMattos et al., 2001), I treated microcultures of RGCs in parallel with GCM or with cholesterol at the same concentration (5 µg/ml) as in GCM (Mauch et al., 2001).

3.1.1 Time course of GCM- and cholesterol-induced changes in the number of synapses

As a first step, measurements in the lab (D Mauch & FW Pfrieger) showed how fast GCM and cholesterol enhance the level of synaptic activity in RGCs, by measuring spontaneous, asynchronous and evoked EPSCs. As shown in Fig. 4, cholesterol and GCM raised the frequencies of spontaneous and asynchronous release and the size of miniature and evoked EPSCs to the same extent and with a similarly slow time course, leading to significant changes after three or more days of treatment.

This raised the question whether cholesterol- and GCM enhanced the number of synapses with the same time course. To resolve this question, I added GCM or cholesterol to five day old microcultures of RGCs and examined after different periods of treatment the number of synapses in neurons growing singly or in small groups on microislands of PDL. Control cells were cultured for the entire period in defined culture medium. Synapses were defined as double labeled puncta, positive for the presynaptic marker synapsin I and the postsynaptic marker GluR2/3. A semi-automated routine analysed the density of immunostained puncta in neurites of RGCs. As shown in Fig. 5, GCM and cholesterol enhanced the number of synapsin-, GluR2/3-positive and of double-stained puncta per neurite area with remarkably similar time courses. As for the effects on synaptic activity shown in Fig. 4, statistically significant changes were reached only after three or more days of treatment.

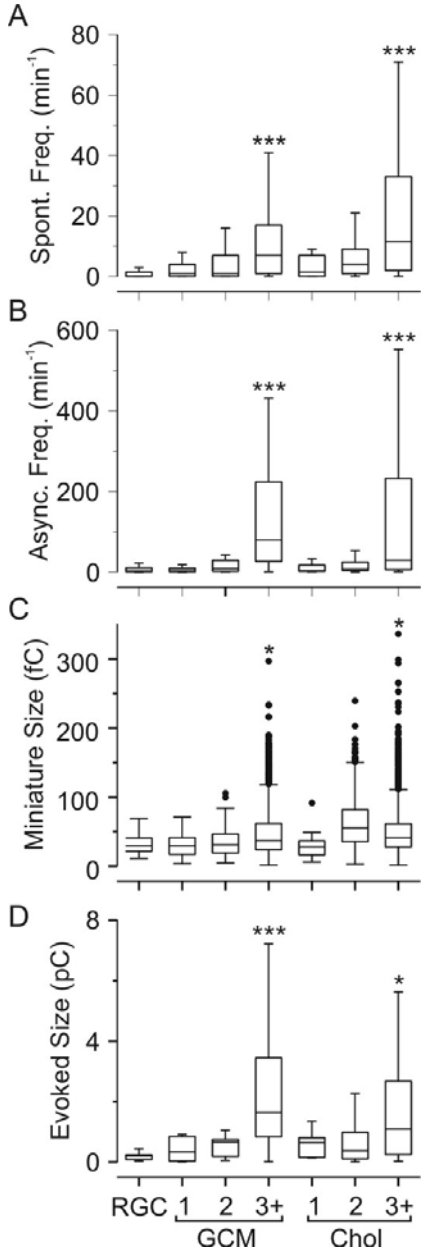

Figure 4: GCM- and cholesterol-induced enhancement of synaptic activity requires at least three days of treatment. Boxplots showing the frequencies of spontaneous (A) and asynchronous EPSCs (B) in RGCs cultured for five days in defined medium and then for 1, 2 or 3 to 7 (3+) days in defined medium (RGC; 60 neurons with activity out of 97 tested), in the presence of GCM (1: 18 of 28; 2: 19 of 34; 3+: 101 of 124) or in the presence of cholesterol (Chol; 1: 14 of 30; 2: 25 of 35; 3+: 112 of 136). In boxplots, horizontal lines represent the median; lower and upper box limits, 1st and 3rd quartile; whiskers, 1.5-fold interquartile range. (C) Charge transfer amplitudes of miniature EPSCs (quantal size) in RGCs cultured as described above in defined medium (RGC; 7 neurons/28 events), in GCM (1: 5/23; 2: 7/105; 3+: 28/901) or in cholesterol (Chol; 1: 5/33; 2: 7/909; 3+: 29/2127). Filled circles indicate values outside the 1.5-fold interquartile range. (D) Charge transfer of evoked EPSCs in RGCs cultured as described above in defined medium (RGC; n = 14 neurons), in GCM (1: 10; 2: 9; 3+: 71) or in cholesterol (Chol; 1: 7; 2: 14; 3+: 67). Asterisks indicate statistically significant changes compared to control cultures (* $p < 0.05$, ** $p < 0.01$, *** $p < 0.001$; A, B: Kruskal-Wallis test; C, D: ANOVA, Dunnett's post-hoc test). Data were recorded by D. Mauch.

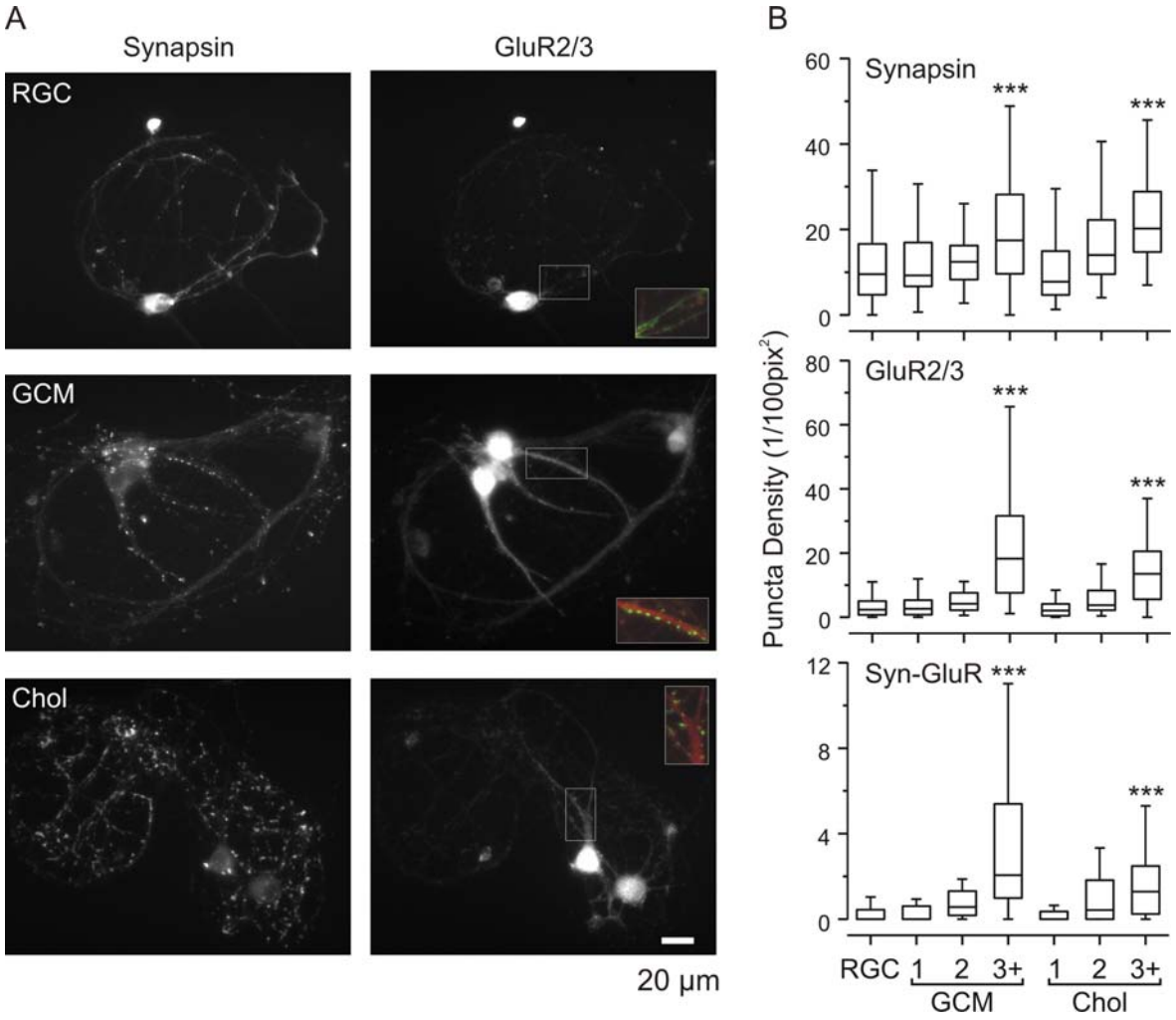

Figure 5: GCM- and cholesterol-induced increase in synapse density requires at least three days of treatment. (A) Fluorescence micrographs of RGCs cultured for five days in defined medium and then for six days in defined medium (top), with GCM (middle) or with cholesterol (bottom) and then stained with antibodies against synapsin I (left column) and GluR2/3 (right column). Inserts show overlays of synapsin I (green) and GluR2/3 (red) fluorescence in indicated areas at 1.5-fold magnification. (B) Densities of synapsin- (top), GluR2/3- (middle) and synapsin-GluR2/3-positive (bottom) puncta on neuritic processes of RGCs cultured for five days in defined medium and then for 1, 2 or at least 3 days in defined medium (RGC; n = 99 neurons), in GCM (1: 31; 2: 21; 3+: 54) or in cholesterol (Chol; 1: 32; 2: 21; 3+: 55). Three or more days of treatment with GCM or cholesterol induced statistically significant changes compared to untreated controls (ANOVA, Dunnett's post-hoc test).

I noted two differences between cholesterol- and GCM-treated cells: First, cholesterol induced a significant, but smaller increase in synapse number than GCM. Second, in cholesterol-treated cultures, synapsin-positive puncta were distributed all over neurites, whereas after treatment with GCM these puncta clustered at distinct spots along neurites.

Taken together, GCM and cholesterol enhanced the number of synapses and their spontaneous and evoked activity not immediately, but slowly within several days of treatment. Cholesterol induced a smaller increase in synapse number than GCM, but mimicked all of the GCM effects on synaptic activity.

3.1.2 Time course of GCM- and cholesterol-induced increase in neuritic cholesterol content

The long-delay, with which both GCM and cholesterol promoted synaptogenesis, contrasted with the notion that synapses form within an hour (Ahmari et al., 2000; Friedman et al., 2000; Gomperts et al., 2000) and suggested that both activated an unknown rate-limiting process. As a first candidate, I tested whether the neuronal uptake of cholesterol causes the delay. Using staining with filipin, a fluorescent sterol-binding antibiotic, Mauch et al., (2001) had shown previously that GCM and cholesterol strongly enhance the level of cholesterol in RGCs. Now, I determined the time course of this effect. As shown in Fig. 6, GCM enhanced the cholesterol content of neurites gradually reaching a 10-fold enhancement within 72 hours. Directly added cholesterol had the same effect, but with a strikingly different time course: It caused a 20-fold increase within 48 hours, which then declined to a remarkably similar level as with GCM after 72 hours. The different time courses are probably caused by the different ways of how cholesterol enters neurons: cholesterol contained in GCM is taken up by (regulated) endocytosis of apolipoprotein E-containing lipoproteins, whereas cholesterol that is directly added to the medium is transferred in an unregulated manner to cells by albumin, a component of the culture medium (Brown and Goldstein, 1986). The subsequent decrease in cellular cholesterol content between 48 and 72 hours, by directly added cholesterol, may be due to active cholesterol release from RGCs to protect them from cholesterol overload.

The different rates of cholesterol- and GCM-induced increase in cholesterol content contrasted with the rather similar delay by which both enhanced synapse numbers. This indicated that the increase in cholesterol content does not determine the rate of synaptogenesis.

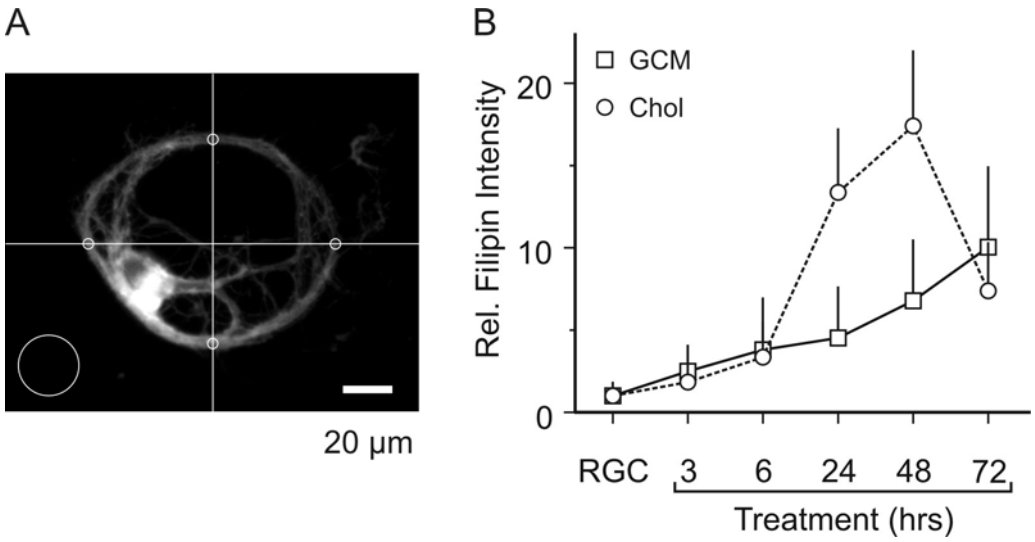

Figure 6: Time course of GCM- and cholesterol-induced increase in neuritic cholesterol content. (A) Fluorescence micrograph of a RGC cultured for five days in defined medium and then for 48 hrs with GCM. Subsequently, the culture was fixed and stained with filipin. Circles indicate regions, where filipin intensity was determined in neurites (small, intersections with center lines) and in background (large). (B) Relative mean intensities of filipin fluorescence in neurites of RGCs cultured for five days in defined medium and then for the indicated times with GCM (black rectangles, solid line; RGC: n = 173 cells; 3: 36; 6: 40; 24: 37; 48: 39; 72: 28) or with cholesterol (red circles, dashed line; RGC: 110; 3: 33; 6: 34; 24: 23; 48: 23; 72: 44). Fluorescence intensities for each time point were normalized to intensities of untreated control cells (RGC). Whiskers indicate standard deviation.

3.1.3 Dendrite differentiation as rate-limiting step for GCM- and cholesterol-induced synaptogenesis

Searching for the rate limiting step in GCM- and cholesterol-induced synaptogenesis, I closer inspected the GluR2/3 immunostaining. This revealed that GCM and cholesterol treatment strongly increased the density of GluR2/3 in neurites, whose tapering form reminded of dendrites (Fig. 5). This observation prompted me to test, whether RGCs formed dendrites in microcultures and whether their development causes the delay in synapse formation. Immunostaining with a MAP2-specific antibody revealed that after 10 to 14 days under control conditions less than 20% of the RGCs tested showed MAP2-positive dendrites (Fig. 7). On the other hand, the majority of RGCs showed MAP2-positive somata and multiple, long and extensively branching neurites extending from their soma (Fig. 7 and Fig. 8). This implied that under control conditions, RGCs grow multiple neurites, but that none of them differentiates into MAP2-positive dendrites. This may

explain the low density of GluR2/3 in neurites (Fig. 5), since glutamate receptors are selectively targeted to mature dendrites (Craig et al., 1993). As next step I treated microcultures with cholesterol or GCM for different periods and counted the number of MAP2-positive dendrites per soma. Both, GCM and cholesterol increased the fraction of RGCs with one or more MAP2-positive dendrites reaching statistically significant changes compared to control cultures after three or more days of treatment (Fig. 7). This time course was remarkably similar to the slow increase in synapse number indicating that dendrite differentiation limits the rate and extent of synaptogenesis in RGCs.

GCM and cholesterol may have increased the content of MAP2 in neurites by enhancing its expression. However, immunoblots of cell extracts showed that RGCs synthesize MAP2 and GluR2/3 under glia free condition and that GCM or cholesterol did not enhance their protein levels (Fig. 9). I also studied whether GCM or cholesterol change the phosphorylation status of MAP2 at sites that have been implicated in neurite outgrowth (Berling et al., 1994; Sanchez et al., 2000), using specific antibodys against MAP2 phosphorylation at serine 136 in the N-terminal region and threonine 1620/1623 in the proline-rich region. As shown in Fig. 9, the phosphorylation status of MAP2 at these sites didn't change within 48 hours of GCM or cholesterol treatment.

Even in the presence of GCM or cholesterol, about 20% of neurons lacked dendrites. Previous observations showed that RGCs impede dendrite development in neighboring cells (Perry & Linden, 1982; Eysel et al., 1985). To determine whether a similar effect occurred in microcultures of RGCs, I counted MAP2 positive dendrites, differentiating between singly growing cells and those with contact to neighbors. Indeed, I found that the percentage of RGCs lacking MAP2-positive dendrites was fourfold higher in neurons growing with one or more neighbors (43%) than in those growing singly on a microisland (12%) indicating an inhibitory effect of neighboring RGCs (Fig. 10).

Together, these results indicate that the low incidence of synapses in RGCs under glia-free conditions is due to a lack of dendrite differentiation. GCM and cholesterol promoted this process, which acted as rate-limiting step for the increase in synapse number and which involved a redistribution of MAP2 and GluR2/3 from the soma to dendrites.

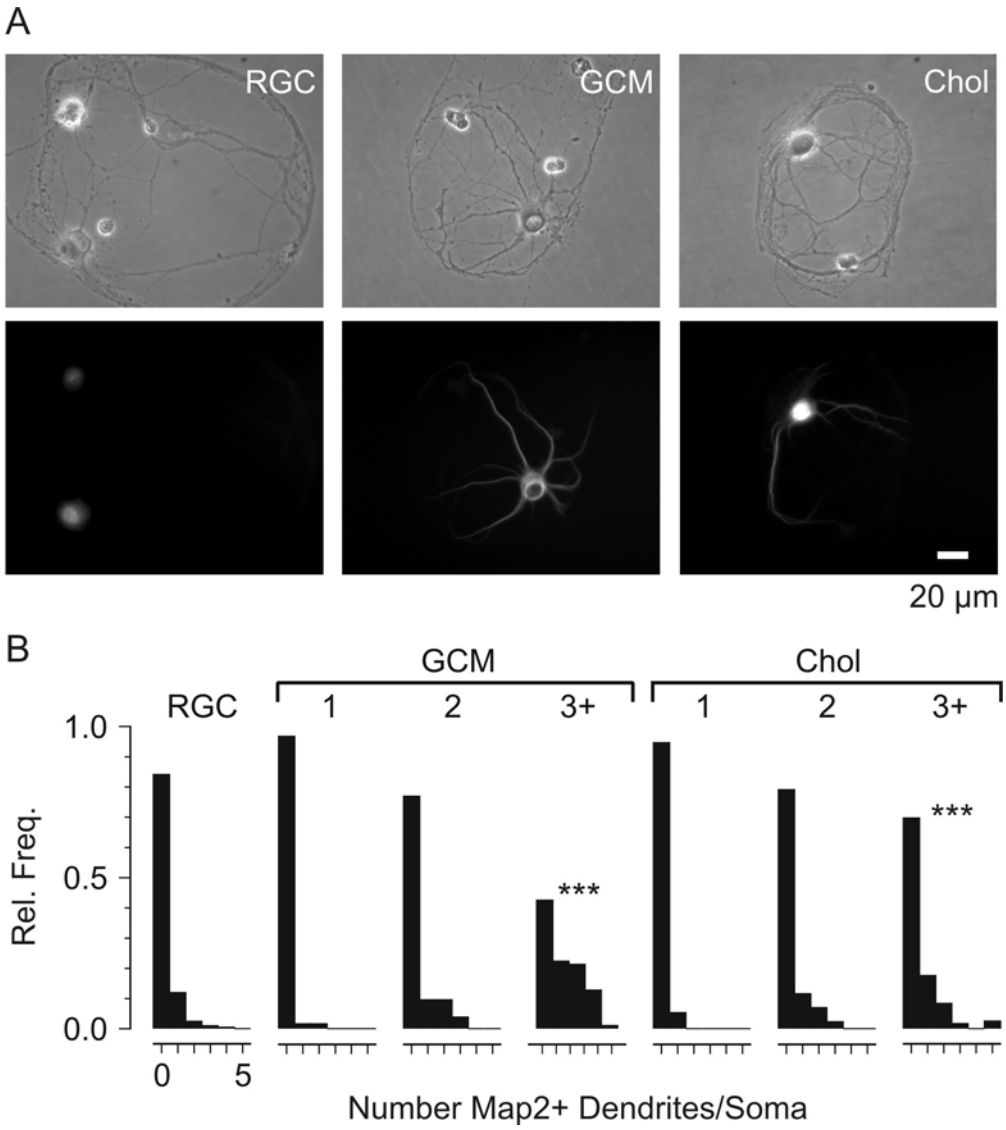

Figure 7: Dendrite formation limits the rate of GCM- and cholesterol-induced synaptogenesis. (A) Phase-contrast (top) and fluorescence (bottom) micrographs of RGCs growing for five days in defined medium and then for three days in defined medium (left), in GCM (middle) and in cholesterol (right). Cultures were stained with antibodies against the dendritic marker MAP2. (B) Relative frequency histograms of the number of MAP2-positive dendrites per soma in RGCs cultured for five days in defined medium and then for 1, 2 or at least 3 days in defined medium (RGC; n= 138 neurons), in GCM (1: 20; 2: 27; 3+: 77) or in cholesterol (Chol; 1: 26; 2: 25; 3+: 91). Only three or more days of treatment with GCM or cholesterol induced statistically significant changes compared to untreated cultures (Pearson's χ^2 test).

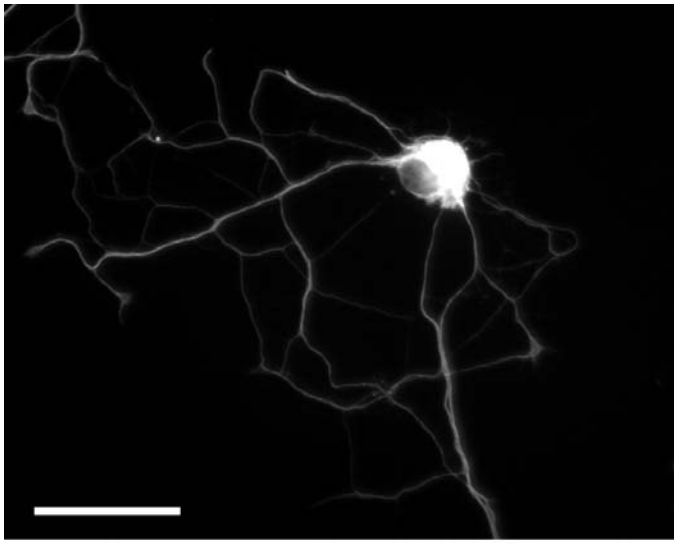

Figure 8: RGCs extend several long, branching processes in the absence of glia-derived factors. Fluorescence micrograph of a representative RGC cultured for seven days in defined medium and then stained with a tubulin-specific antibody. Space bar, 50 µm.

3.1.4 Evidence for laminin as dendrite-promoting factor

Cholesterol induced a statistically significant increase in the number of MAP2-positive dendrites, but it was less efficient than GCM. This may explain the lower number of synapses in cholesterol- compared to GCM-treated RGCs. Both observations indicated that other glial signals may promote dendrite differentiation. Based on previous studies, I tested whether the matrix component laminin induces dendrites. A first hint to laminin came from the study of Meyer-Franke et al. (1995), observing MAP2-positive dendrites in cultures of immunoisolated rat RGCs, but their neurons were plated on laminin-2 (merosin), whereas the microcultures which I used contained PDL. Second, it is well established that laminins are secreted by astrocytes (Liesi et al., 1983; Selak et al., 1985) and promote neurite outgrowth in RGCs and other neurons (Baron-Van Evercooren et al., 1982; Manthorpe et al., 1983; Rogers et al., 1983; Luckenbill-Edds, 1997; Powell & Kleinman, 1997). Treatment of five day old microcultures for three days with a low concentration of laminin-1 (0.25 µg/ml) did not change the number of MAP2-positive dendrites per neuron compared to untreated control. However, addition of laminin-1 together with cholesterol increased dendrite differentiation to a very similar degree as GCM (Fig. 11). Laminin-2, which was originally used by Meyer-Franke et al. (1995), fully mimicked this effect (data combined with them for laminin-1, Fig. 11).

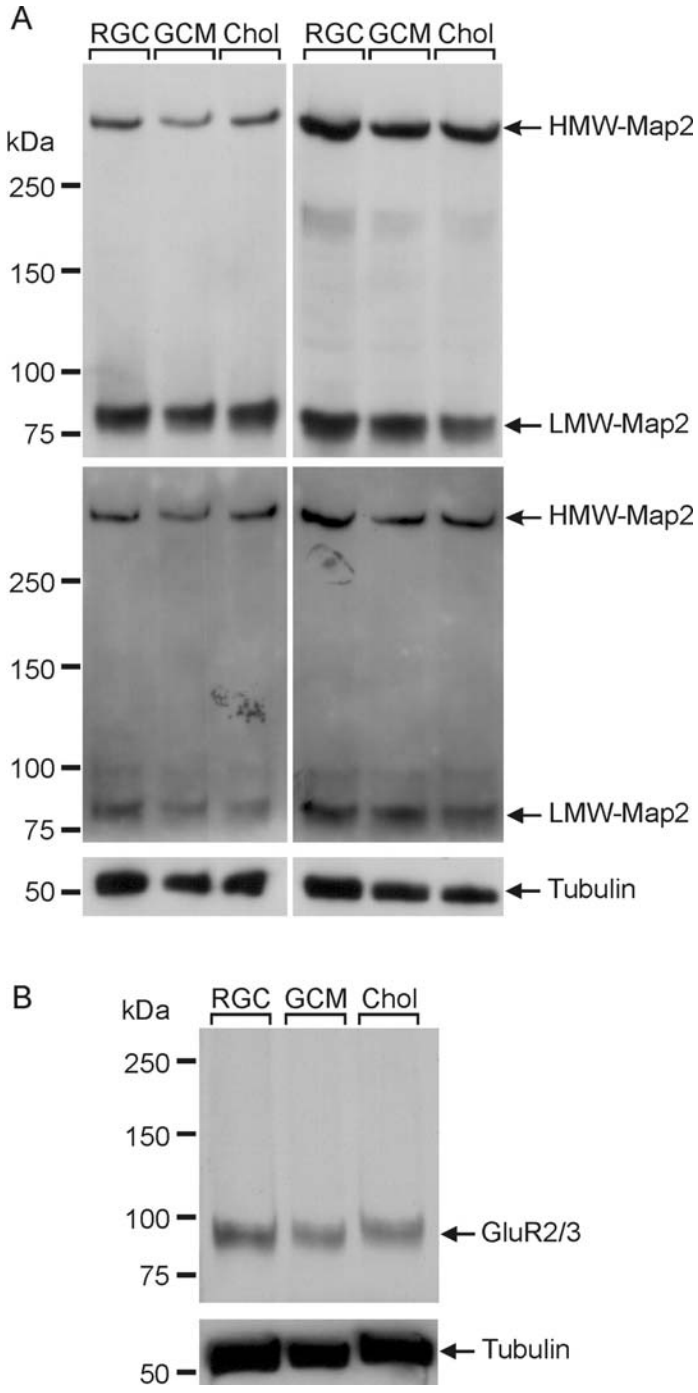

Figure 9: GCM or cholesterol do not change MAP2 and GluR2/3 levels. (A) Immunoblots of RGCs growing for 4 days in defined medium and then for 2 days in the presence of defined medium (RGC), GCM or cholesterol using antibodies against specific phophorylation sites (top left, thr1620/23; top right, ser136), total MAP2 (middle panel, stripped blots from top panel) and against tubulin (bottom). Arrows indicate high molecular weight (HMW) and low molecular weight (LMW) MAP2. (B) Immunoblot of RGCs cultured for 4 days in defined medium and then for 6 days in the presence of defined medium (RGC), GCM or cholesterol using an antibody against GluR2/3 (top) and tubulin (bottom).

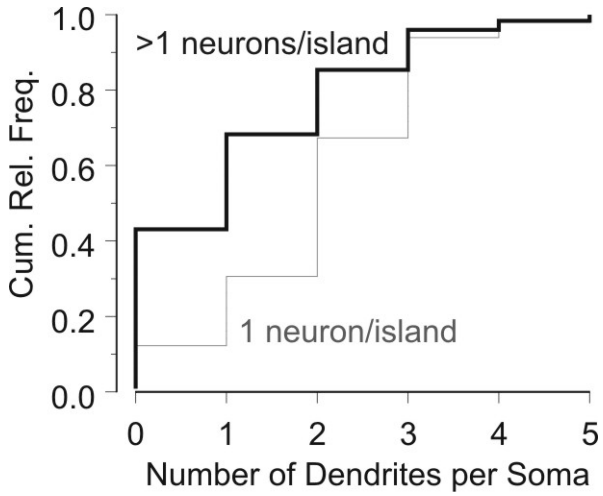

Figure 10: Neighboring RGCs suppress dendrite differentiation in RGCs. Cumulative relative frequency plot of the number of MAP2-positive dendrites per soma for RGCs growing singly on microislands (thin line; n = 49 neurons) or together with at least one more neuron (thick black line; n = 123 neurons). The two distributions differ significantly ($p < 0.001$; Pearson's χ^2 test). Cells grew for four days under defined conditions and then for 4 to 6 days in the presence of GCM.

Laminins are trimers consisting of α, β and γ chains (Burgeson et al., 1994) and so I tested next which laminin chain mediates the effect. I treated microcultures with synthetic peptide fragments from different laminin chains which are known to enhance neurite growth (Liesi et al., 1989; Sephel et al., 1989). The dendrite-promoting activity of laminin-1 was selectively mimicked by a fragment from the γ1 chain, but not by a fragment from the long arm of the α1 chain (Fig. 11). These observations are in line with the results, that both laminin-1 and -2, which have different α chains, promote dendrite differentiation. Immunoblots confirmed that laminin-γ1 is present in GCM (Fig. 12) at relatively high concentrations (5 to 10 µg/ml). My attempts to deplete laminin from GCM by immunoprecipitation using a polyclonal antibody against laminin 1+2, or to block its effects by addition of this antibody to GCM before treatment of RGCs failed, probably due to the high concentration and its effectiveness at low doses.

Together, these results showed that RGCs require cholesterol to form mature dendrites and that laminins promote dendritogenesis via the γ1 chain.

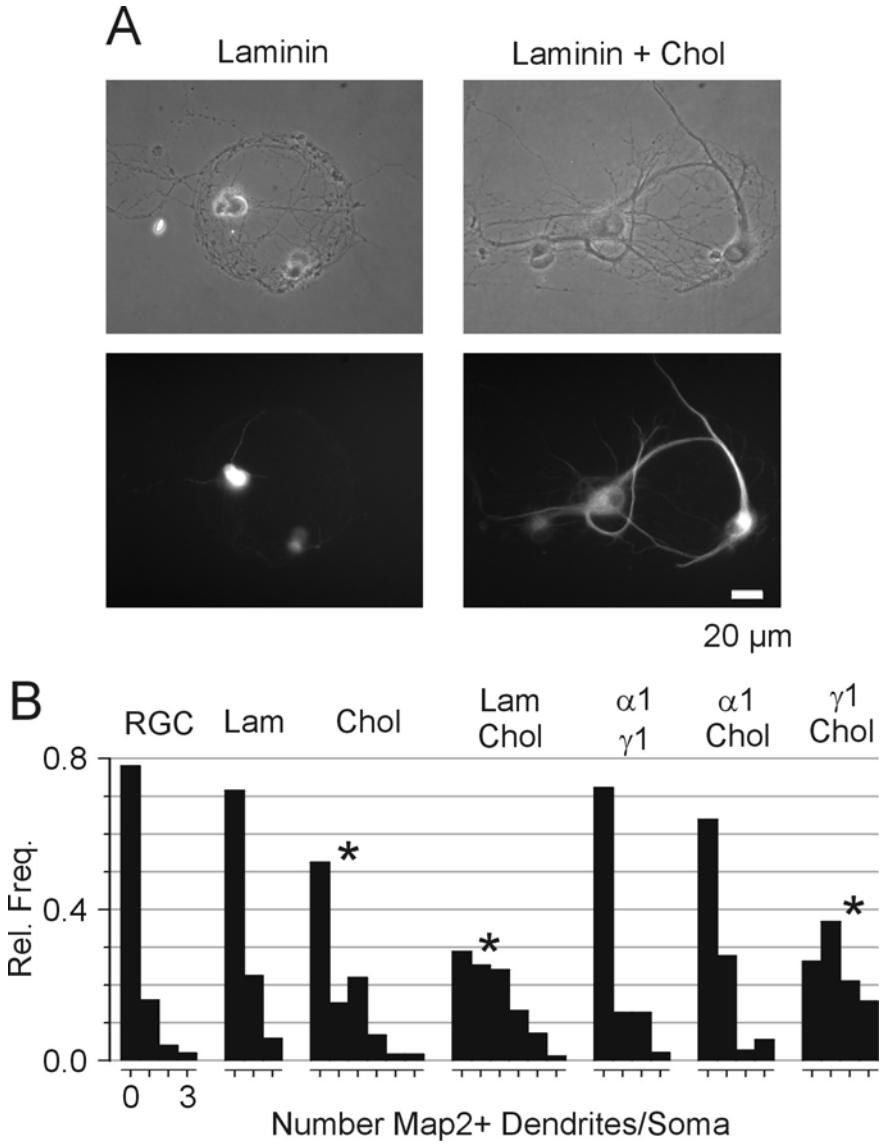

Figure 11: Dendritogenesis requires cholesterol and is promoted by laminin. (A) Phase-contrast (top) and fluorescence (bottom) micrographs of RGCs growing for five days in defined medium and then for three days in defined medium plus laminin (left) or plus laminin (250 ng/ml) and cholesterol (5 µg/ml) (right). Cultures were stained with a MAP2-specific antibody. Space bar, 20 µm. (B) Relative frequency histograms of the number of MAP2-positive dendrites per soma of RGCs cultured for four days in defined medium and then for at least 3 days in defined medium (RGC, untreated control; n = 50 cells), with laminin (250 ng/ml; n = 102), with cholesterol (5 µg/ml; n = 59; $p < 0.05$), with laminin and cholesterol (n = 83; $p < 10\text{-}5$), with two fragments from the α1 and γ1 chain (250 ng/ml each; n = 47), with the α1 fragment and cholesterol (n = 36) and with the γ1 fragment and cholesterol (n = 38; $p < 10\text{-}4$). Values for each treatment are from two to four independent preparations. Asterisks indicate statistically significant changes compared to untreated control (Pearson's $\chi 2$ test).

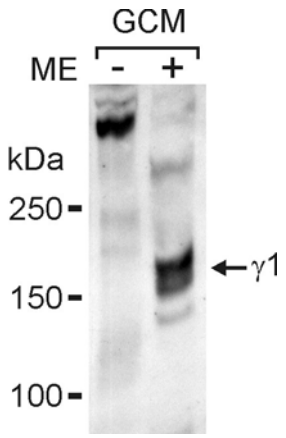

Figure 12: GCM contains a large amount of laminin-γ1. Immunoblot of GCM using an antibody against the laminin-γ1 chain. ME (mercaptoethanol) indicates presence/absence of reducing conditions.

3.1.5 Effects of GCM removal on synaptic activity

So far, the results showed that glial cholesterol and laminin promote dendrite differentiation and the formation of synapses, but it remained unclear, whether these effects persisted after their removal or whether glial factors were required to maintain synaptic activity. Therefore I tested, whether the GCM-induced increase in synaptic activity persisted after removal of GCM.

To address this, RGCs were cultured for four days under control conditions and then treated for five days with GCM to stimulate synapse formation and synaptic activity. At this point, the GCM-induced baseline synaptic activity was recorded (Fig. 13A). Then, GCM was removed, cells were washed once with PBS to remove soluble glial factors and cultured in defined medium or in the presence of GCM or of cholesterol (Fig. 13A). After further six days of culture (total 15 days in vitro), synaptic activity was recorded to detect its sensitivity to the removal of GCM and its replacement by cholesterol. I observed that in those RGCs, where GCM was removed, the frequency of spontaneous and asynchronous release and the quantal size remained at the baseline level (Fig. 13). In those cultures, where GCM treatment was continued, the frequencies of spontaneous and asynchronous release increased further (Fig. 13) and this increase persisted also, if GCM was replaced by cholesterol (Fig. 13). This indicated that RGCs continue to form synapses in vitro, if provided with cholesterol. Remarkably, removal of GCM caused a significant decrease in the size of evoked EPSCs below the baseline level and a significant increase in the fraction

of neurons, where stimulation failed to evoke EPSCs (Fig. 13). Again, these changes did not occur, when GCM was replaced by cholesterol (Fig. 13).

Taken together, these results showed that the continuous presence of cholesterol is required to maintain evoked synaptic transmission and to support ongoing synaptogenesis.

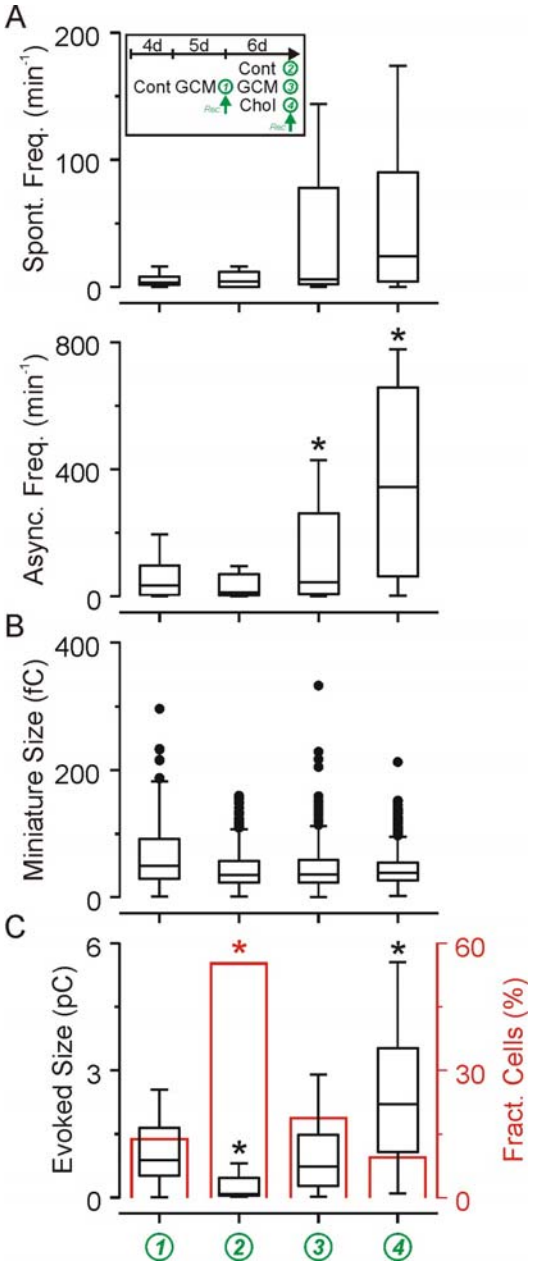

Figure 13: Effects of GCM removal on synaptic activity. (A) insert: Timing of culture treatment and electrophysiological recordings. Immunoisolated RGCs were cultured for 4 days in defined medium and for 5 days with GCM. Then, synaptic activity was recorded to define GCM-induced baseline activity (1). GCM was washed off with PBS and replaced by defined culture medium, GCM or medium plus cholesterol. After six more days, synaptic activity was recorded to define the effects of GCM removal (2), of the continued presence of GCM (3) or of its replacement by cholesterol (4) on synaptic activity. Boxplots in (A) show frequencies of spontaneous (upper panel) and asynchonous (lower) EPSCs. (B) Charge transfer amplitudes of miniature EPSCs. (C) Charge transfer amplitudes of evoked EPSCs (left axis, black boxplots) and fraction of neurons showing spontaneous or asynchronous events but no evoked EPSCs (right axis, red columns). After removal of GCM, the size of evoked EPSCs and the fraction of neurons lacking EPSCs decreased and increased compared to the baseline, respectively. Continued treatment with GCM or cholesterol prevented this decrease. Asterisks indicate statistically significant changes compared to baseline (A, C left axis: Kruskal-Wallis test; C right axis: Pearson's χ^2 test).

3.2 Influence of soluble glial factors and cholesterol on gene expression of cultured postnatal RGCs

So far, I had shown that glia-derived laminin and cholesterol are necessary for dendrite differentiation in purified RGCs, and that this step probably acts rate limiting for synapse formation. Apart from this effect, soluble glial factors may affect further aspects of RGC differentiation. In order to search for new neuronal targets which are influenced by soluble glial signals, I studied the influence of glial factors on RGC gene expression. To separate the influence of cholesterol from that of other soluble glia factors, I compared gene expression in purified RGCs after 30 hours of treatment with GCM or cholesterol with untreated control cells. To study a broad range of genes, I performed gene chip expression analysis using the Affymetrix system, which allows to investigate expression changes of several thousand genes at once. All experiments concerning the gene chip hybridization, data read out and processing were done in the University Hospital of Regensburg in cooperation with the group of Prof. Gerd Schmitz.

3.2.1 Microarray analyses and data assessment

Gene chip arrays are highly sensitive tools. For stringency, control analyses were performed at all steps of sample preparation. First, prepared sample RNA was analyzed for degradation using capillary electrophoresis. Fig. 14A shows the separation profile of total RNA purified from control RGCs as an example. The diagram shows three peaks, a standard peak at 17 seconds, the 18 S rRNA at 35 and the 28 S rRNA at 41 seconds. Both rRNA peaks are clearly distinguishable and no degradation fragments are present. Fig. 14B shows the electrophoresis profile of purified cDNA after reverse transcription of mRNA using T7-oligo(dT) primer. For microarray hybridization, labeled RNA fragments were generated by reverse transcription of cDNA using T7 polymerase and biotin-labeled ribonucleotides followed by metal induced statistical fragmentation. Fig. 14C shows the size distribution of fragmented antisense RNA. Labeled antisense RNA fragments were hybridized on oligonucleotide microarrays (Affymetrix rat expression set 230), representing 31.000 probe sets including 28.000 identified rat genes and ESTs.

The variability of expression data between independent experiments is a critical point and determines their reliability. I performed cross correlation analysis of the hybridization signals of the three independent experiments after GCM treatment as well as under the

corresponding control conditions (Fig. 15). Correlation coefficients ranged between 0.96 and 0.985, showing a high data stability across experiments.

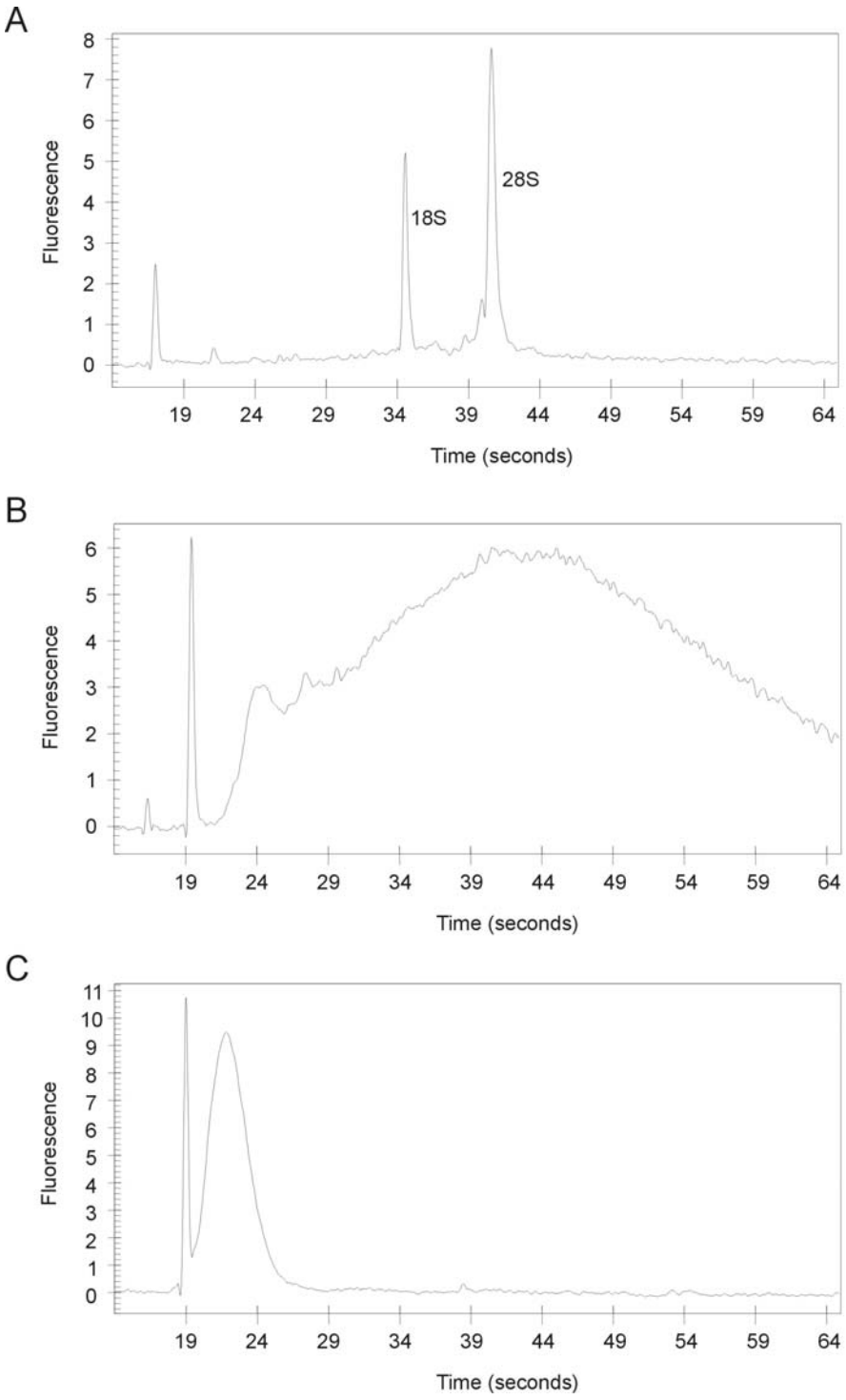

Figure 14: Quality control at different steps of sample preparation: (A) Electrophoretic separation profile of control sample RNA, standard peak at 17 seconds, 18 S rRNA at 35 seconds and 28 S rRNA at 41 seconds. (B) Electrophoresis profile of purified cDNA after reverse transcription. (C) Size distribution of fragmented antisense RNA.

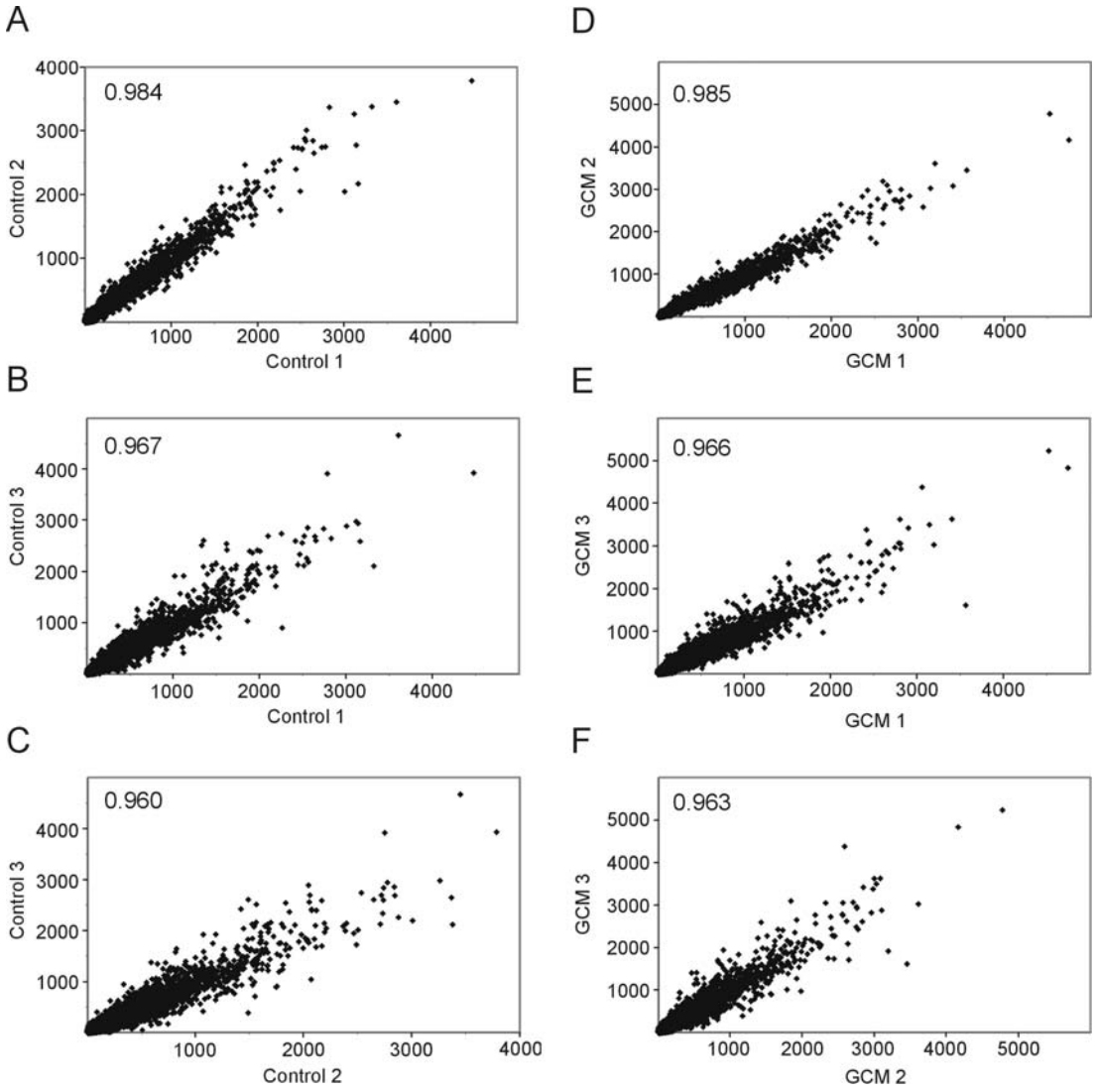

Figure 15: Microarray data are highly reproducible across experiments.
Cross-correlation of hybridization signals. (A-C) Hybridization signals for control RGCs in three independent experiments. (D-F) Hybridization signals for GCM-treated RGCs in three independent experiments. Numbers indicate correlation coefficients.

To detect relevant gene expression changes I set four criteria: First, only genes were selected which are present under control conditions - in the case of downregulation, or under treated conditions - in the case of upregulation, over all three experiments. Second, up- or downregulation of a single gene occurred in all of the three experiments. Third, the mean fold change over all three experiments was higher than 1.34 fold. And fourth, the CV for each gene over the three independent experiments was below 0.6. All genes which fulfilled these criteria were grouped by their function or cellular localization. Exceptions from these criteria were only made in special cases of known relevance as indicated.

3.2.2 Expression changes in RGCs related to soluble glia derived factors

GCM treatment of cultured RGCs for 30 hours resulted in changes of 82 genes, given in table 6. In general, gene regulation occurred in both directions and regulated genes were associated with different functional groups. The regulated genes were involved in sterol biosynthesis and regulation of cholesterol homeostasis, steroid metabolism, fatty acid synthesis, regulation of transcription, growth- and neurotrophic factors, extracellular matrix components, signal transduction or cell adhesion, for example (Tab. 6). The ten most downregulated genes mediated cholesterol synthesis and homeostasis, fatty acid synthesis, and steroid metabolism. On the other side, the top ten upregulated genes were distributed over several functional groups.

Table 6: Gene expression changes in cultured RGCs after 30h of GCM treatment

Gene	Trend	Fold change	CV	Sequence derived form
Sterol biosynthesis and regulation of cholesterol homeostasis				
mevalonate pyrophosphate decarboxylase	↓	3.48	0.16	NM_031062
growth response protein (CL-6) / insulin induced gene 1 (Insig1)	↓	2.3	0.41	NM_022392
acetyl-Coenzyme A acetyltransferase 2 (Acat2)	↓	2.3	0.25	AI412322
isopentenyl-diphosphate delta isomerase	↓	2.24	0.44	NM_053539
farensyl diphosphate synthase	↓	2.14	0.32	NM_031840
farnesyl diphosphate farnesyl transferase 1 / squalene synthase	↓	2	0.36	NM_019238
2,3-oxidosqualene lanosterol cyclase	↓	1.95	0.18	BM390574
cytochrome P450, subfamily 51	↓	1.91	0.36	NM_012941
sterol-C4-methyl oxidase-like	↓	1.87	0.33	NM_080886
3-hydroxy-3-methylglutaryl-Coenzyme A synthase 1 / HMG-CoA synthase, soluble	↓	1.87	0.27	NM_017268
ESTs, similar to Delta(14)-sterol reductase [Rattus norvegicus]	↓	1.78	0.15	BM390364
ESTs, similar to 24-dehydrocholesterol reductase (DHCR24) [Homo sapiens]	↓	1.74	0.27	BF417479
mevalonate kinase	↓	1.74	0.27	AW433971
acetyl-CoA acetyltransferase / thiolase	↓	1.7	0.06	NM_023104
ESTs, similar to low density lipoprotein receptor [Mus musculus]	↓	1.66	0.46	BI294974
squalene epoxidase	↓	1.66	0.46	NM_017136
3-hydroxy-3-methylglutaryl-Coenzyme A reductase / HMG CoA reductase	↓	1.59	0.19	BM390399
phenylalkylamine Ca2+ antagonist (emopamil) binding protein / 3-beta-hydroxysteroid-delta-8,delta-7-isomerase	↓	1.59	0.19	NM_057137
sterol-C5-desaturase (fungal ERG3, delta-5-desaturase)-like	↓	1.48	0.08	AB052846
ESTs, highly siminlar to sterol regulatory element binding protein-2 (SREBP-2) [Cricetulus griseus]	↓	1.41	0.86*	AI170663
7-dehydrocholesterol reductase	↓	1.41	0.16	NM_022389
ATP-binding cassette, sub-family G (WHITE), member 1	↑	1.48	0.79*	NM_053502

Gene	Trend	Fold change	CV	Sequence derived form
Steroid metabolism				
ESTs, similar to hydroxysteroid dehydrogenase 17 beta, type 7 (Hsd17b7) [Mus musculus]	↓	2.09	0.09	AI176172
ESTs, weakly similar to steroidogenic acute regulatory protein precursor homolog [Homo sapiens]	↓	2.05	0.18	AI236580
ESTs, highly similar to NAD(P) dependent steroid dehydrogenase-like / aldo-keto reductase family 1, member C4 [Mus musculus]	↓	1.62	0.2	BF407232
Fatty acid synthesis				
stearoyl-Coenzyme A desaturase 1	↓	2.24	0.21	J02585
fatty acid synthase	↓	1.55	0.07	AI179334
fatty acid desaturase 1	↓	1.52	0.27	NM_053445
stearoyl-Coenzyme A desaturase 2	↓	1.48	0.36	BE107760
Thyroid hormone responsive protein (spot14)	↓	1.45	0.49	NM_012703
fatty acid elongase 2	↓	1.35	0.11	BE116152
phosphate cytidyltransferase 2, ethanolamine	↓	1.35	0.29	NM_053568
Energy metabolism				
isocitrate dehydrogenase 1	↓	1.52	0.14	NM_031510
ATP citrate lyase	↓	1.35	0.22	NM_016987
Regulation of transcription / Chromatin associated				
ESTs, similar to E2F transcription factor 3 [Mus musculus]	↑	1.52	0.59	AI060205
ESTs, similar to Wilms tumor 1 associated protein (WTAP) [Mus musculus]	↑	1.52	0.36	AA900400
cysteine-rich protein 3	↑	1.45	0.58	NM_057144
ESTs, highly similar to Thymidylate kinase/deoxythymidylate kinase (DTYMK) [Mus musculus]	↑	1.41	0.33	BI290898
ESTs, similar to interferon regulatory factor 2 (IRF2) [Mus musculus]	↑	1.38	0.53	BI302791
ESTs, similar to modulator of estrogen induced transcription [Rattus norvegicus]	↑	1.35	0.44	BF397936
ESTs, similar to putative transcription factor ZNF131 [Rattus norvegicus]	↑	1.35	0.54	BE110637
Neurotransmission				
transient receptor potential cation channel, subfamily C, member 3 (Trpc3)	↓	1.38	0.53	NM_021771
G protein-coupled receptor 51 / GABA-B receptor 2	↑	1.45	0.39	NM_031802
Growth- and neurotrophic factors				
pancreatitis-associated protein 1 / Reg2	↑	1.55	0.07	NM_053289
ESTs, similar to insulin-like growth factor I [Mus musculus]	↑	1.38	0.36	BE103520
Extracellular matrix components				
matrix Gla protein	↑	2.58	0.28	NM_012862
Tissue inhibitor of metalloproteinase 3	↑	1.38	0.36	AI599265
EST, weakly similar to nidogen 1 (Nid1) [Mus musculus]	↑	1.38	0.53	AI070991
Cytoskeleton organization				
ESTs, similar to platelet-activating factor acetylhydrolase 45kD subunit (Pafah) / lissencephaly-1 protein (LIS-1) [Mus musculus]	↓	1.82	0.52	BG663460
ESTs, weakly similar to actopaxin [Rattus norvegicus]	↓	1.35	0.29	AA899471
kinesin family member 3c	↑	1.38	0.51	BF553488

Gene	Trend	Fold change	CV	Sequence derived form
Protein synthesis, modification transport and degradation				
ESTs, similar to E3 ligase for inhibin receptor [Rattus norvegicus] or HECT domain containing 1 (Ubiquitin-protein ligase) [Mus musculus]	↓	1.45	0.47	AW531948
ESTs, similar to syntaxin 11 (Stx11) [Mus musculus]	↓	1.41	0.28	AW920037
ESTs weakly similar to ribosomal protein S23 [Rattus norvegicus]	↑	1.55	0.37	BE114185
ESTs, moderately similar to polypeptide GalNAc transferase T1 [Rattus norvegicus]	↑	1.41	0	AI103845
ESTs, moderately similar to CGI-09 protein [Homo sapiens]	↑	1.38	0.27	BF560079
Signal transduction				
diazepam binding inhibitor	↓	1.48	0.44	AI175009
ESTs, moderately similar to membrane-spanning 4-domains, subfamily A, member 10 [Mus musculus]	↓	1.45	0.32	AI555523
ESTs, similar to galanin receptor 2 (Galr2) [Mus musculus]	↓	1.35	0.29	AI385327
ESTs, serine/threonine kinase 32C (Stk32c) [Mus musculus]	↓	1.35	0.44	BE097305
interleukin 24	↑	1.35	0.11	NM_133311
ESTs, similar to Rho GTPase activating protein 12 [Rattus norvegicus] / Rho guanine nucleotide exchange factor (Larg) [Mus musculus]	↑	1.35	0.47	AI137762
Cell adhesion				
ESTs, similar to integrin, beta-like 1 / ten beta-integrin EGF-like repeat domains [Mus musculus]	↓	1.45	0.49	BI303923
ESTs, protocadherin 18 [Mus musculus]	↓	1.38	0.4	BF408099
Stress				
Metallothionein 1	↓	1.35	0.11	AF411318
heme oxygenase 1	↑	1.62	0.31	NM_012580
ESTs, similar to sestrin 2 (Sesn2) [Mus musculus]	↑	1.38	0.56	BE109653
Immune response				
ESTs, hypothetical Immunoglobulin and major histocompatibility complex domain containing protein	↓	1.41	0.57	BI294746
ESTs, highly similar to toll-like receptor 1 [Mus musculus]	↓	1.38	0.53	AI070419
ESTs, T-cell receptor alpha/delta locus [Mus musculus]	↓	1.38	0.44	BE098148
Other functions				
ESTs, highly similar to cora cornifin alpha (small proline-rich protein 1) (SPRR1) [Rattus norvegicus]	↑	1.38	0.1	BI286387
ESTs, highly similar to atda diamine acetyltransferase / Spermidine/spermine N(1)-acetyltransferase (SSAT) / Putrescine acetyltransferase [Mus musculus]	↑	1.38	0.2	AA893220
ESTs, moderately similar to HSPC133 protein (DC3) [Homo sapiens]	↑	1.35	0.47	BE113965
Unknown function				
ESTs, similar to nasopharyngeal carcinoma susceptibility protein [Rattus norvegicus] or ankyrin repeat-containing cofactor-1 (ANCO1) [Homo sapiens]	↓	1.48	0.46	BE097847

Gene	Trend	Fold change	CV	Sequence derived form
ESTs, highly similar to T9S3_MOUSE Transmembrane 9 superfamily protein member 3 precursor [Mus musculus]	↓	1.45	0.23	BF545305
ESTs, highly similar to nucleolar protein GU2 [Mus musculus]	↓	1.38	0.2	AI170715
ESTs, similar to male sterility protein 2-like protein [Torpedo marmorata]	↓	1.38	0.2	AI555210
ESTs, similar to EGF-like module containing, mucin-like, hormone receptor-like sequence 1 [Mus musculus]	↓	1.38	0.1	BE100625
ESTs, similar to MYOSIN-IXA homolog [Homo sapiens]	↓	1.35	0.22	AW535406
ESTs, similar to nasopharyngeal epithelium specific protein 1 [Rattus norvegicus]	↑	1.52	0.49	BF419626
ESTs, similar to lymphocyte antigen 6 complex [Mus musculus]	↑	1.41	0.59	BE108597
ESTs, similar to hypothetical Esterase/lipase/thioesterase family active site containing protein [Mus musculus]	↑	1.38	0.44	AI603103

Table 6: Gene expression changes in RGCs after 30 hours of GCM treatment. Arrows indicate up- (↑) or down- (↓) regulation compared to control. Italized genes are similarly regulated by cholesterol treatment. Stars (*) indicate CV values which are larger than the threshold.

3.2.2.1 GCM regulated cholesterol synthesis and homeostasis in cultured RGCs and caused downregulation of genes involved in steroid metabolism and fatty acid synthesis

The largest functional group of regulated genes concerned cholesterol homeostasis. All investigated genes encoding for enzymes directly involved in cholesterol biosynthesis were downregulated. In addition, the cholesterol synthesis regulating protein INSIG, the cholesterol esterification enzyme Acat2, the cholesterol uptake mediating LDL receptor and the sterol regulatory element binding protein 2 (SREBP-2) were downregulated. On the other hand, the cholesterol releasing ABC transporter G1 (ABC-G1) was upregulated by GCM treatment. These results indicated that GCM treatment diminished neuronal cholesterol synthesis and uptake and enhanced cholesterol release.

To confirm these results on the protein level, I selected squalene synthase (SQS) as the key enzyme at the entrance of the cholesterol synthesis pathway, whose gene was two-fold downregulated. GCM treatment of microculture RGCs drastically reduced the protein level of SQS as shown by immunostaining using a specific antibody against SQS (Fig. 16). For direct evidence of neuronal cholesterol synthesis regulation, I performed labeling of newly synthesized cholesterol using a radioactive precursor. RGCs were incubated with ^{14}C-acetat as cholesterol precursor in absence or presence of GCM. After 48 hours of

incubation, lipids were extracted and separated by TLC. Fig. 17 shows the autoradiogram of the labeled lipid profile. Visible as clear band in line with the cholesterol standard, cultured RGCs synthesized cholesterol under the given culture conditions and GCM treatment reduced this de novo synthesis drastically.

To confirm the upregulation of the ABC-G1, I performed quantitative real time RT-PCR in cooperation with the group of Prof. Gerd Schmitz in Regensburg. After five days in culture, RGCs were cultured in the presence of GCM for further five days before RNA was prepared. Analysis by real time PCR revealed a 3.46 fold higher mRNA level for ABC-G1 under GCM treated conditions compared to control cells. Since ABC-G1 is known to be involved in cholesterol and phospholipid efflux (Schmitz et al., 2001), I tested next if the expression enhancement of ABC-G1 is correlated to neuronal cholesterol release. Performing pulse chase labeling using ^{14}C-acetat as lipid precursor followed by lipid analysis of the culture media of untreated and GCM treated RGCs (Fig. 18), I showed that GCM treatment increased the release of endogenous cholesterol to the culture medium compared to untreated conditions. Additionally, treatment with GCM caused also neuronal phosphatidylcholine release.

In addition to the large group of genes mediating cholesterol homeostasis, down-regulated genes were involved in steroid- and fatty acid biosynthesis. Steroid synthesis requires cholesterol as common precursor and partially shares enzymes and regulatory pathways with cholesterol synthesis. The steroidogenic acute regulatory protein (STAR) transports cholesterol from the outer- to the inner mitochondrial membrane where the first steroidogenic enzyme P450scc is localized (Thomson, 2003; Stocco, 2001) but also oxysterol producing enzymes such as cholesterol 27-hydroxylase (Sugawara et al., 1995) which have a significant impact in the regulation of cholesterol metabolism. The two other genes in his group are hydroxysteroid dehydrogenase 17 beta and aldo-keto reductase 1C4.

Fatty acid synthesis is similar transcriptional regulated as cholesterol synthesis, and both pathways were activated by the transcription factor SREBP-1a (Horton et al., 2002). Several key genes involved in fatty acid synthesis and regulation were downregulated by GCM. In addition to fatty acid synthesizing enzymes like fatty acid synthase, -desaturase 1 and -elongase 2, the thyroid hormone responsive protein – responsible for the activation of genes encoding for enzymes of fatty acid synthesis was downregulated by 1.45 fold.

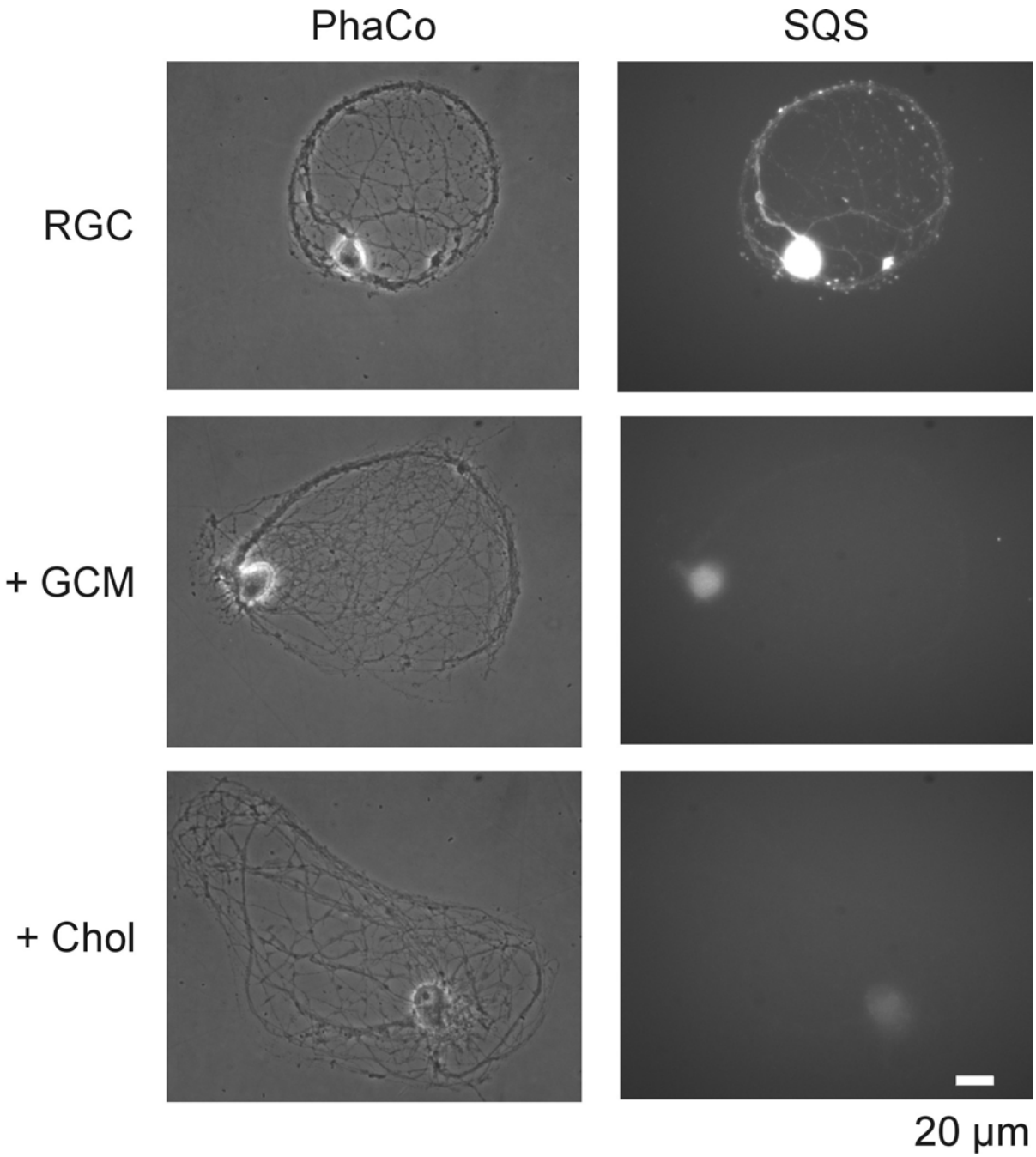

Figure 16: GCM- and cholesterol-induced downregulation of SQS
Phase-contrast (left) and fluorescence (right) micrographs of RGCs, which were cultured for six days in defined medium and then for five days in defined medium (RGC), with GCM or with cholesterol and which were then stained with an antibody against SQS.

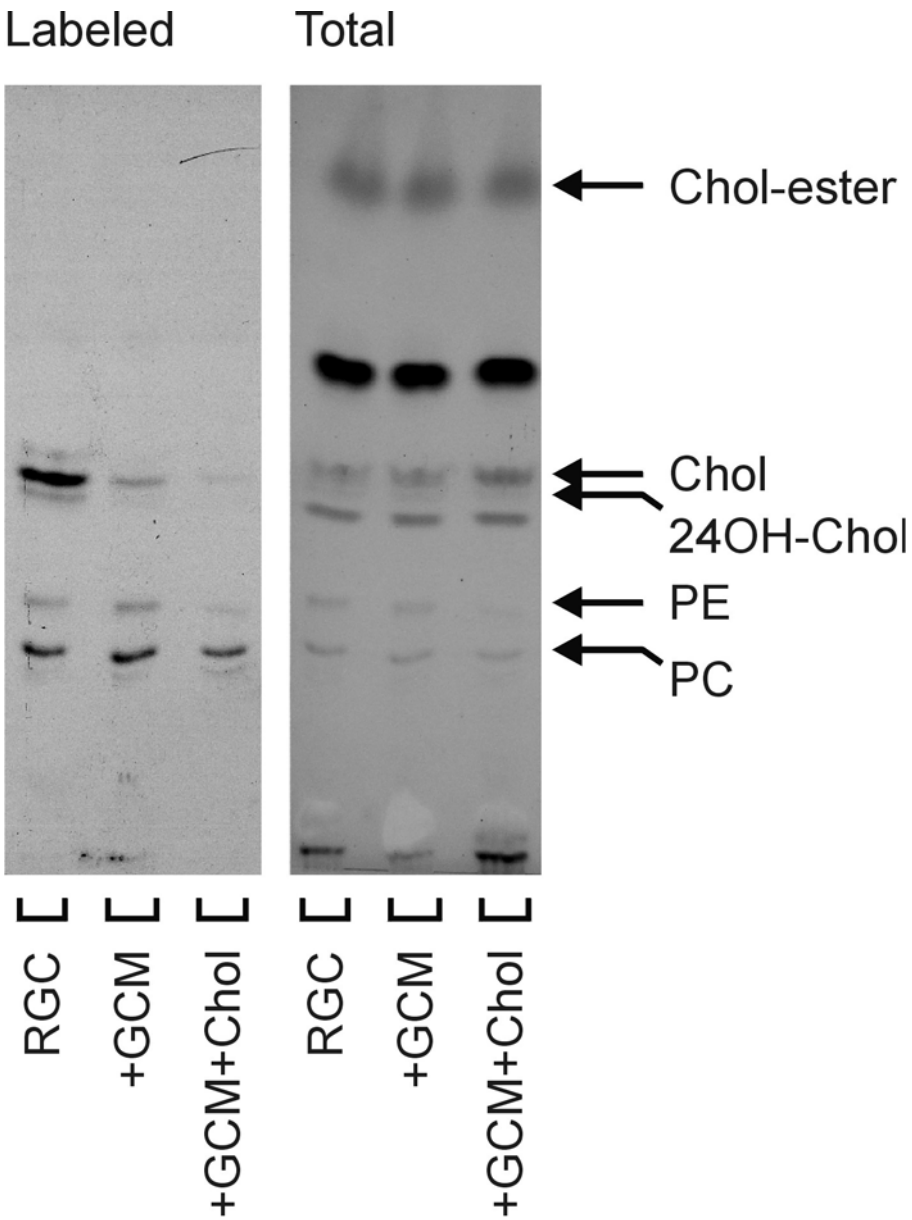

Figure 17: GCM-induced downregulation of cholesterol synthesis in RGCs.
Micrographs show the autoradiogram (left) and total lipid staining (right) of the same TLC plate. RGCs were cultured for seven days in defined medium and then for 48 hours in defined medium (RGC), with GCM or with GCM + cholesterol in the presence of ^{14}C-acetat as cholesterol precursor. Lipids were extracted by hexan/isopropanol from cells and separated by TLC. Arrows indicate positions of lipid standards running together with samples: Chol – cholesterol; 24OH-chol – 24-hydroxy-cholesterol; PE – phosphatidylethanolamine; PC – phosphatidylcholine. Chol-ester – cholesteryl-ester. TLC by K. Nieweg.

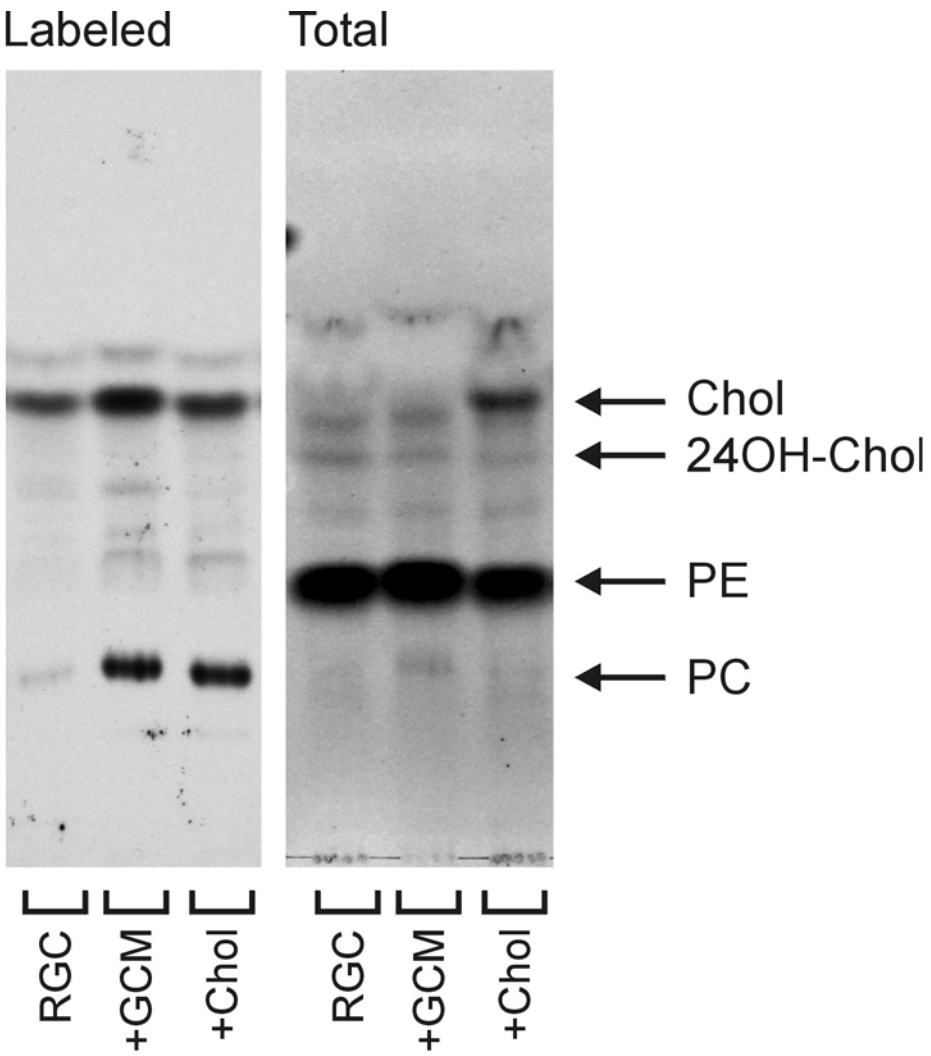

Figure 18: GCM- and cholesterol-induced endogenous cholesterol and phosphatidylcholine release of RGCs.

Micrographs show the autoradiogram (left) and total lipid staining (right) of the same TLC plate. RGCs were cultured for seven days in defined medium and then for 48 hours in defined medium in presence of ^{14}C-acetat as lipid precursor. After washing, cells were cultured for 48 hours in defined medium (RGC), with GCM or with cholesterol. Lipids were extracted by chloroform/methanol from culture medium and separated by TLC. Arrows indicate positions of lipid standards running together with samples: Chol – cholesterol; 24OH-chol – 24-hydroxy-cholesterol; PE – phosphatidylethanolamine; PC – phosphatidylcholine.

Together, these results demonstrated that GCM downregulated the cholesterol biosynthesis in cultured RGCs as shown on gene expression-, protein- and lipid level. Treatment with GCM enhanced the expression of the ABC-G1 transporter and led to endogenous cholesterol and phosphatidylcholine release. Further, genes involved in steroid metabolism and fatty acid synthesis were downregulated by GCM treatment.

3.2.2.2 GCM upregulates matrix Gla protein and heme oxygenase 1 in cultured RGCs

In the following, I will focus on the two most upregulated genes. The highest upregulated neuronal gene in response to GCM treatment encodes for the MGP, a small ubiquitous matrix protein (Price & Williamson, 1985; Luo et al., 1995). This gene is 2.58 fold up-regulated with a small CV (0.28).

A first experiment to localize MGP in RGCs was performed with untreated cells and cells that were treated for five days with GCM, using immunostaining with a specific antibody. Immunofluorescence showed an association of MGP with somata and dendrites of GCM treated RGCs as demonstrated by double labeling with the dendritic marker MAP2, whereas control cells showed only stained somata (Fig. 19).

The second highly upregulated neuronal gene in response to GCM treatment encoded for heme oxygenase 1 (HO1). It showed a change of 1.62 fold and a CV of 0.31. HO1 is a well known enzyme that cleaves the heme ring at the alpha methene bridge to form biliverdin, ferric iron and carbon monoxide (CO) (Tenhunen et al., 1968).

The expression upregulation could be confirmed on protein level. Immunoblotting using a specific antibody against HO1, showed for GCM-treated dense culture RGCs an upregulation of HO1 after three days of treatment compared to control (Fig. 20). Furthermore, intracellular localization of HO1 was investigated by double labeling of microculture RGCs using specific antibodies against HO1 and GluR2/3 (Fig. 21). RGCs growing for five days in defined medium and then for four days in defined medium with GCM, showed a similar distribution for HO1 and GluR2/3 positive staining in somata and dendrites. Control cells, which were cultured for the whole time in defined medium, showed only somata association of HO1 and GluR2/3.

Taken together, the upregulation of MGP and HO1 could be confirmed on the protein level. Both proteins showed dendritic localization.

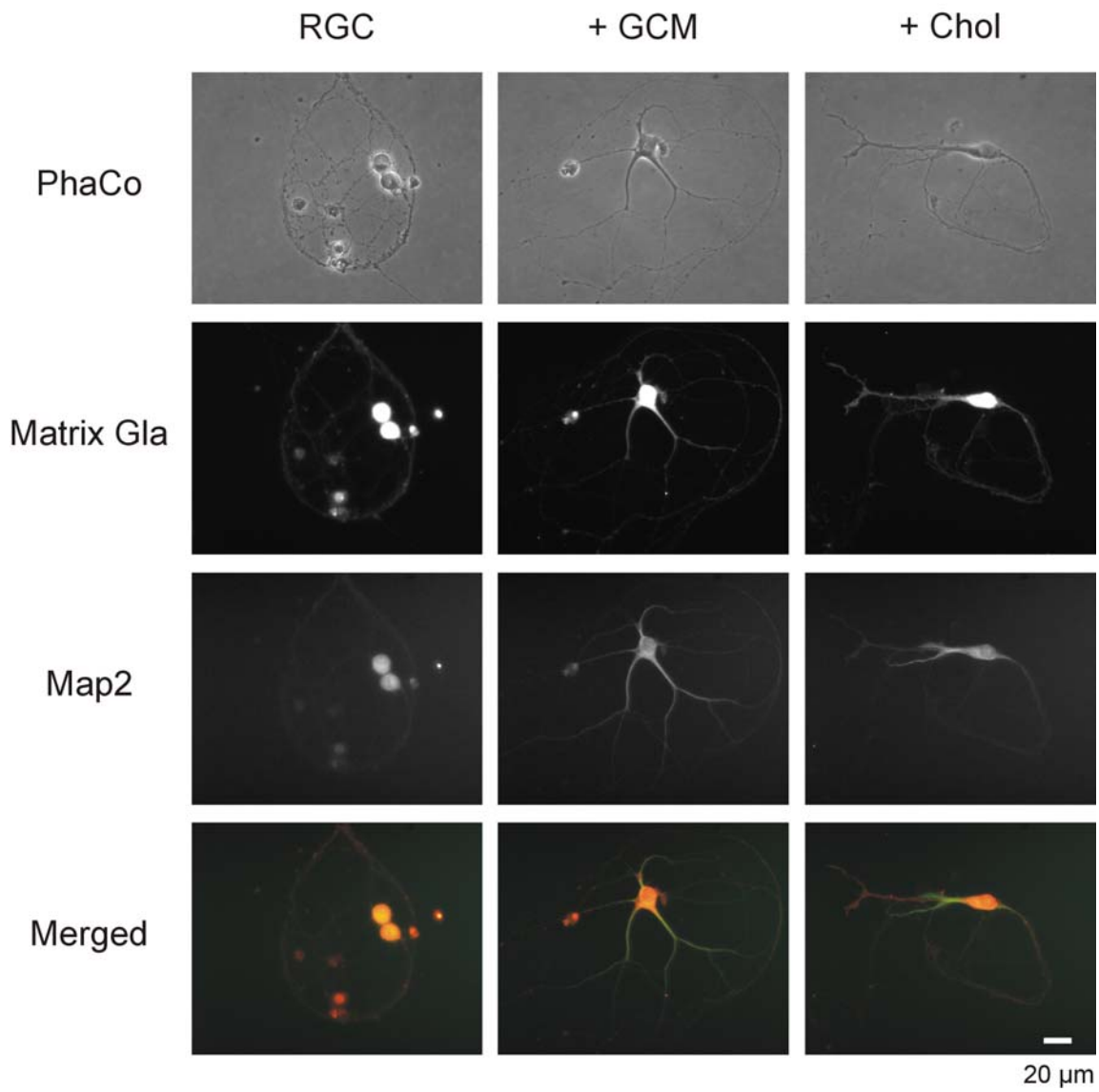

Figure 19: Localization of MGP in RGCs.

Phase-contrast and fluorescence micrographs of RGCs growing for three days in defined medium and then for five days in defined medium (left), with GCM (middle) and with cholesterol (right). Cultures were stained with antibodies against MGP and the dendritic marker MAP2. Merged images show MGP in red and MAP2 in green.

3.2.3 Comparison of GCM and cholesterol-induced expression changes

As shown before, cholesterol itself has a profound influence on RGC differentiation. To search for neuronal genes that mediate these effects and to distinguish the influence of cholesterol from other glial factors, I treated cultured RGCs for 30 hours with cholesterol at the same concentration as it is present in GCM and compared the gene expression pattern with that of untreated control cells. I found that directly added cholesterol regulated the gene expression of 37 genes, given in table 7. As for GCM, regulated genes were associated with different functional groups like sterol biosynthesis and regulation of cholesterol homeostasis, splicing, extracellular matrix components, signal transduction, stress reaction and vesicle transport (Tab. 7).

A comparison of genes that were regulated by cholesterol and GCM treatment showed that the expression of 18 genes changed in a similar manner. These genes belonged exclusively to the functional groups of sterol biosynthesis and regulation of cholesterol homeostasis, steroid metabolism and fatty acid synthesis.

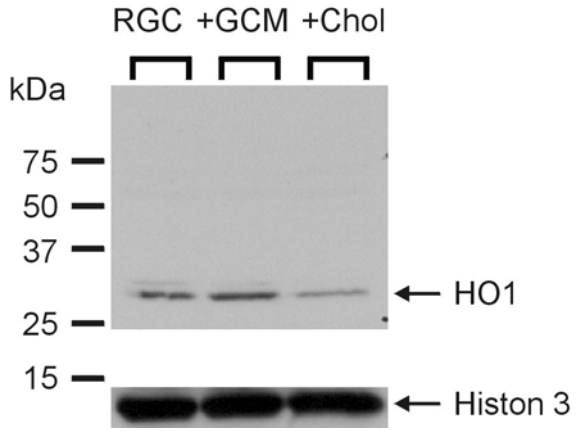

Figure 20: Differential regulation of HO1 by GCM and cholesterol.
Immunoblot of RGCs growing for four days in defined medium and then for three days in the presence of defined medium (RGC), GCM or cholesterol using antibodies against HO1 and Histon 3 (bottom).

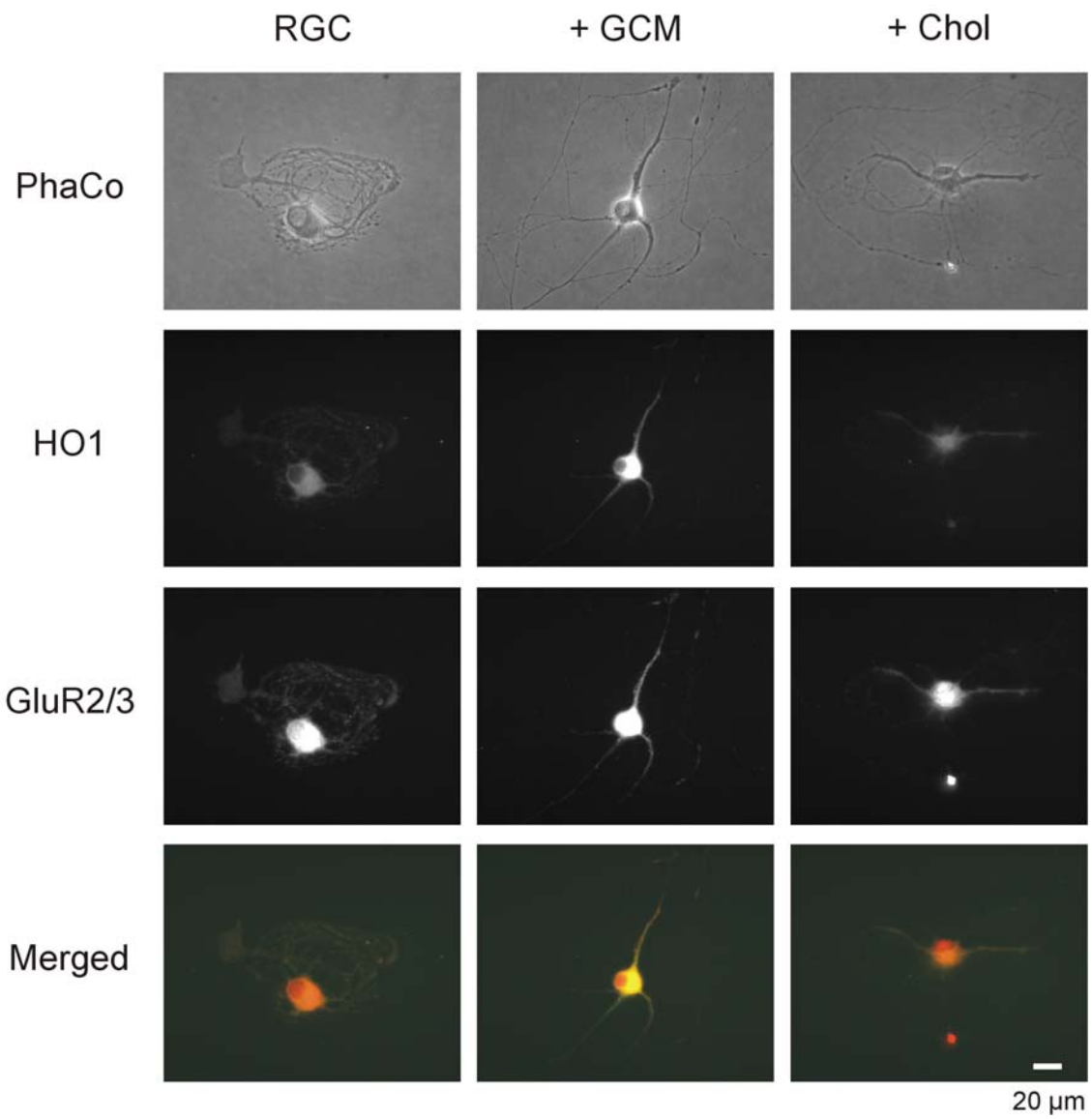

Figure 21: Localization of HO1 in RGCs.

Phase-contrast and fluorescence micrographs of RGCs growing for three days in defined medium and then for five days in defined medium (left), with GCM (middle) and with cholesterol (right). Cultures were stained with antibodies against HO1 and the postsynaptic marker GluR2/3. Merged images show HO1 in green and GluR2/3 in red.

Table 7: Gene expression changes in cultured RGCs after 30h of cholesterol treatment

Gene	Trend	Fold change	CV	Sequence derived form
Sterol biosynthesis and regulation of cholesterol homeostasis				
isopentenyl-diphosphate delta isomerase	↓	2.0	0.14	BI290053
mevalonate pyrophosphate decarboxylase	↓	1.82	0.24	NM_031062
growth response protein (CL-6) / insulin induced gene 1 (Insig1)	↓	1.7	0.33	NM_022392
2,3-oxidosqualene: lanosterol cyclase	↓	1.55	0.52	BM390574
sterol-C4-methyl oxidase-like	↓	1.52	0.49	NM_080886
cytochrome P450, subfamily 51	↓	1.52	0.49	NM_012941
squalene epoxidase	↓	1.48	0.3	NM_017136
7-dehydrocholesterol reductase	↓	1.48	0.36	NM_022389
acetyl-Coenzyme A acetyltransferase 2 (Acat2)	↓	1.48	0.44	AI412322
acetyl-CoA acetyltransferase / thiolase	↓	1.45	0.09	NM_023104
mevalonate kinase	↓	1.41	0.57	NM_031063
3-hydroxy-3-methylglutaryl-Coenzyme A synthase 1 / HMG-Co A synthase, soluble	↓	1.38	0.53	NM_017268
farnesyl diphosphate farnesyl transferase 1 / squalene synthase	↓	1.38	0.53	NM_019238
ESTs, similar to low density lipoprotein receptor [Mus musculus]	↓	1.38	0.66*	BI294974
farnesyl diphosphate synthase	↓	1.35	0.61*	NM_031840
3-hydroxy-3-methylglutaryl-Coenzyme A reductase / HMG-CoA reductase	↓	1.35	0.47	BM390399
Steroid metabolism				
hydroxysteroid dehydrogenase 17 beta, type 7	↓	1.45	0.09	NM_017235
Fatty acid synthesis				
stearoyl-Coenzyme A desaturase 1	↓	1.45	0.64*	J02585
ESTs, highly similar to hypertension-associated protein SA [Rattus norvegicus]	↓	1.38	0.36	BI282211
Energy metabolism				
pyruvate dehydrogenase phosphatase isoenzyme 2	↓	1.41	0.49	AF062741
ESTs, Weakly similar to lactate dehydrogenase D [Mus musculus]	↑	1.38	0.56	AI501131
Chromatin associated / splicing				
ESTs similar to Transformer-2 protein homolog (TRA-2 ALPHA) homolog [Homo sapiens]	↑	1.48	0.22	AI137236
ESTs, similar to SMC4 protein homolog/ Structural maintenance of chromosomes 4-like 1 protein [Microtus arvalis],	↑	1.41	0.59	AW535494
ESTs similar to FUS interacting protein (serine-arginine rich) 1 / TLS-associated protein with SR repeats (TASR)	↑	1.41	0.59	AI070564
ESTs similar to Histone deacetylase 8 (Hdac8) [Mus musculus]	↑	1.35	0.29	BE117008
Neurotransmission				
ESTs similar to glutamate receptor, ionotropic, N-methyl-D-aspartate 3A [Homo sapiens]	↑	1.35	0.29	AI146055
Extracellular matrix components				
netrin 1	↑	1.59	0.37	NM_053731

Gene	Trend	Fold change	CV	Sequence derived form
Cytoskeleton organization				
ESTs, Highly similar to autophagy 5-like [Mus musculus]	↑	1.52	0.36	AW528235
rapostlin	↑	1.41	0.33	BE105446
calpain 8 (Capn8)	↑	1.41	0.49	NM_133309
Signal transduction				
ESTs, similar to Serine/threonine-protein kinase nek1 (NimA-related protein kinase 1) [Mus musculus]	↓	1.38	0.36	AI406369
neuraminidase 3	↑	1.45	0.39	NM_054010
receptor-like tyrosine kinase	↑	1.35	0.54	AB073721
ESTs, Moderately similar to FMT_MOUSE Methionyl-tRNA formyltransferase, mitochondrial precursor (MtFMT) [Mus musculus]	↑	1.35	0.39	AW251803
Stress				
selenoprotein P, plasma, 1	↑	1.48	0.08	AA799627
Vesicle transport				
ESTs, Moderately similar to golgi autoantigen, golgin subfamily a, 4 (Golga4), [Mus musculus]	↑	1.35	0.54	BF568007
Unknown function				
ESTs, Highly similar to CGI-67 serine protease [Rattus norvegicus]	↑	1.62	0.58	AI007882

Table 7: Gene expression changes in RGCs after 30h of cholesterol treatment. Arrows indicate expression up- (↑) or down- (↓) regulation compared to control. Stars (*) indicate CV values which are larger than the threshold.

3.2.3.1 Cholesterol treatment mimicked the GCM induced reduction of neuronal cholesterol synthesis

Similar to GCM, cholesterol treatment caused a downregulation of the sterol synthesis pathway, as well as the downregulation of Acat2 and LDL receptor. Immunostaining for SQS (Fig. 16) as well as radioactive labeling with ^{14}C-acetat as cholesterol precursor (Fig. 17) confirmed cholesterol-induced downregulation of neuronal cholesterol synthesis and of enzymes. The release of endogenous cholesterol by exogenous cholesterol treatment was lower as for GCM (Fig. 18) and just marginally higher as control level. However, the level of endogenous released phosphatidylcholine was considerable higher as under control conditions and similar to GCM treated RGCs (Fig. 18). Similarities concerning expression regulation of genes involved in steroid metabolism and fatty acid synthesis were limited to the genes of hydroxysteroid dehydrogenase 17 beta and steaoryl-CoA desaturase.

Taken together, these results demonstrated that exogenously added cholesterol regulated cholesterol synthesis in cultured RGCs similar to GCM. This suggests that

cholesterol contained in GCM in form of lipoproteins caused the detected downregulation of neuronal cholesterol synthesis by GCM.

3.2.3.2 Cholesterol did not affect MGP and HO1 gene expression but downregulates HO1 on protein level in RGCs

Comparing upregulated genes by cholesterol and GCM treatment, I observed no overlap between these two groups. Gene expression of MGP, drastically upregulated by GCM, was unaffected by cholesterol treatment. Double labeling of cholesterol-treated microcultures for MGP and MAP2 revealed a redistribution of MGP from somata to dendrites similar as seen for GCM. However, dendritic labeling was weaker as for GCM-treated cells whereas control cells showed only stained somata (Fig. 19).

HO1, which was highly upregulated by GCM, was unaffected by 30 hours of cholesterol treatment. However, immunobloting of cell lysate from dense culture RGCs treated for three days with cholesterol, showed a clear downregulation of HO1 on protein level compared to control (Fig. 20). Further, immunostaining of microculture RGCs cultured for four days in the presence of cholesterol confirmed this result (Fig. 21). This regulation appeared in opposite to the noted GCM effect, where treatment for the same time caused a clear upregulation of HO1. However, the association of HO1 with GluR2/3 at dendrites occurred in both, cholesterol and GCM treated RGCs, indicating a redistribution of HO1 from Somata to dendrites.

Together, MGP and HO1 gene expression was not affected by 30 hours of cholesterol treatment in contrast to GCM. Longer cholesterol and GCM treatment induced opposite effects on HO1 protein levels. GCM enhanced the protein level, whereas cholesterol lowered it. GCM and cholesterol induced redistribution of MGP and HO1 from soma to dendrites.

3.2.3.3 Cholesterol enhanced CGI-67 serine protease and Netrin 1 expression

The highest upregulated gene due to cholesterol treatment was an EST similar to CGI-67 serine protease. It was 1.62 fold regulated and had with 0.58 a relatively high CV. Its identification as serine protease stems from sequence analysis and so far nothing is known about its functional role.

The second highest upregulated gene was netrin 1, where cholesterol caused a fold change of 1.59 at the expression level of RGCs compared to control, at a CV of 0.37. Netrin 1 is known as matrix molecule and involved in axon guidance (see introduction).

Both, CGI-67 and netrin 1 were not regulated by GCM treatment. Together, these results showed that directly added cholesterol at the same concentration as in GCM caused gene expression changes that were distinct from those induced by GCM.